Colloid Polym Sci (2004) 282: 901–909
DOI 10.1007/s00396-004-1117-0

ORIGINAL CONTRIBUTION

Dariush Hinderberger
Gunnar Jeschke
Hans-Wolfgang Spiess

Network formation involving polyelectrolytes in solution: the role of counterions

Received: 6 February 2004
Accepted: 23 March 2004
Published online: 22 April 2004

Dedicated to Professor E.W. Fischer on the occasion of his 75th birthday.

D. Hinderberger · G. Jeschke
H.-W. Spiess (✉)
Max-Planck-Institut für Polymerforschung,
Postfach 3148, 55021 Mainz, Germany
E-mail: spiess@mpip-mainz.mpg.de
Tel.: +49-6131-379-120
Fax: +49-6131-379-320

Abstract The network-forming ability of a small fraction of nanosized trianions of the triarylmethyl class (TAM) with poly(diallyldimethylammonium chloride) (PDADMAC) polyelectrolyte is studied by high-field/high-frequency (≈94 GHz) electron paramagnetic resonance spectroscopy. These tristar-shaped organic ions are expected to undergo both electrostatic and hydrophobic interactions with PDADMAC chains. The dependence of electron spin echo (ESE)-detected spectra of the TAM spin probe on PDADMAC concentration reveals a heterogeneous distribution of the spin-carrying counterions. One fraction of these ions forms densely packed clusters while another one is highly diluted. On varying the concentration ratio of TAM spin probe/PDADMAC, the mean distance between closest neighbors within clusters of approximately 1.5 nm does not change significantly, while their fraction increases with decreasing polyelectrolyte content. These findings indicate that the nanosized organic TAM trianions induce network formation in solutions of PDADMAC polyelectrolyte. The data are consistent with a zip-like cooperative binding effect of TAM ions, making this spin probe an interesting building block for electrostatic self-assembly.

Keywords Polyelectrolyte networks · Physical crosslinks · Cooperative binding · Nanoheterogeneity · EPR spectroscopy

Introduction

Polymers that form three-dimensional networks in solution have been under intense experimental and theoretical investigation for several decades [1, 2, 3] owing to their importance in modern industrial applications (e.g., as superabsorbing materials in diapers or as thickeners in foodstuff [4, 5]) and their potential use in other fields (e.g., as intelligent drug delivery systems in medicine) [6].

The linkers that connect individual polymer chains in such three-dimensional networks can be either covalent or related to some associative interaction (e.g., hydrogen bonding or electrostatic attraction). In the latter case, network formation is reversible, which gives rise to a number of interesting effects. An important class of such reversible network-forming materials are polyelectrolytes [7, 8]. While the macroscopic changes upon network formation, such as high osmotic pressure [7, 9], are characterized and understood in some detail, structure and dynamics of polyelectrolytes in solution [10, 11] and the microscopic processes upon build-up of larger network structures are less well known and still a matter of debate [1, 7, 10].

The topology of the network that is formed depends on the type of bonding or interaction that provides the crosslinks and on conformational constraints of the polymer chains. Accordingly, several mechanisms of build-up of larger, three-dimensional structures have been suggested that differ mainly in the degree of ordering of the chains in the network. Three examples are visualized in Fig. 1. Upon crosslinking, uncharged

amorphous random-coil polymers tend to form statistically linked coils (Fig. 1a). Semicrystalline polymers may physically crosslink via lamellar crystalline domains that are shared by several chains (Fig. 1b) [12]. Networks of shape-persistent polyelectrolytes, whose formation is induced by electrostatic and hydrophobic interactions, may exhibit even higher, macroscopic order (Fig. 1c) [11]. Often such rigid-rod polymers form bundles as a direct consequence of the conformational constraint that acts on them.

For polyelectrolytes, three factors govern conformations in solution as well as the formation and structure of the networks: i) the structure of the chain backbone and distribution of the charges of the polyelectrolyte itself, ii) the nature of the counterions (i.e., the number of charges, charge density, and chemical structure), and iii) the interaction of polyelectrolyte and counterions with the solvent.

We have recently started a systematic investigation of polyelectrolyte–counterion interactions by applying electron paramagnetic resonance (EPR) spectroscopy spin probes [13, 14] as tracers for counterions, mainly focusing on cationic poly(diallyldimethylammonium chloride) (PDADMAC) as polyelectrolyte and the small dianionic spin probe Fremy's salt (FS, potassium nitrosodisulfonate) [15, 16, 17]. In contrast to well-established scattering techniques (light, X-ray, and neutron scattering), EPR spectroscopy on spin-carrying counterions does not depend on a particularly high degree of order and is local, highly sensitive, and highly site-selective. Thus, insight into local phenomena can be obtained that is inaccessible otherwise.

In this publication, we shift the focus from PDADMAC interacting with small, inorganic FS spin probes towards interaction of the same polyelectrolyte with large, organic, tristar-shaped trianions of the triarylmethyl class (TAM, see structures of TAM, FS and PDADMAC in Scheme 1) [18, 19]. In particular the differences in the abilities of the two spin probe counterions with respect to the formation of PDADMAC networks are elucidated.

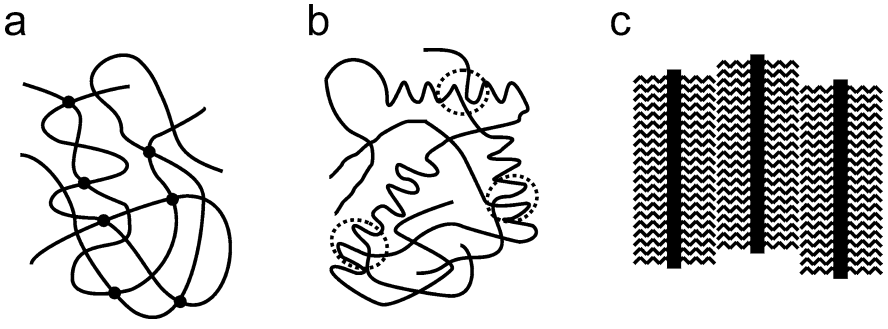

Fig. 1a–c Formation of networks, gels, and aggregates with different degree of order. **a** Covalent network in an amorphous polymer due to chemical crosslinking. **b** Strong physical gel due to formation of microcrystalline domains in which several chains participate. **c** Aggregation of rod-like amphiphilic molecules to bundles due to hydrophobic interaction

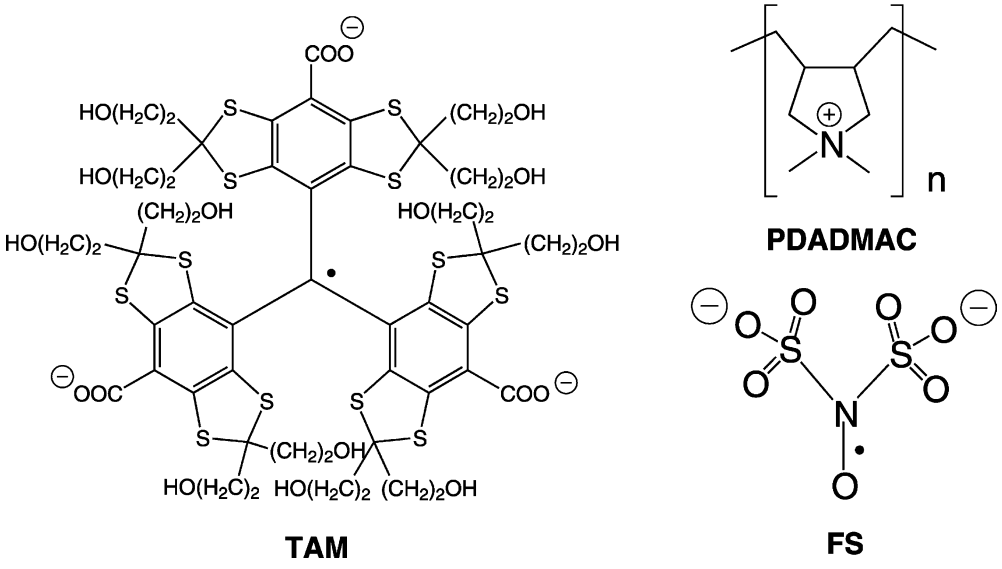

Scheme 1 Molecular structures of the polyelectrolytes and spin probes used in this study. *TAM* triarylmethyl radical trianion (counterions Na^+); *FS* Fremy's salt dianion (counterions K^+, potassium nitrosodisulfonate); *PDADMAC* poly(diallyldimethylammonium chloride)

The paper is organized as follows: we first give an introduction to the spin-probing approach and describe the materials and experimental methods employed in this work. Then, previous experimental results from continuous wave (CW) and Fourier transform (FT) EPR spectroscopy on liquid solutions of PDADMAC with the two different spin probe counterions are briefly reviewed to set a frame of reference for the following discussion of new results from high-field/high-frequency pulse EPR spectroscopy on frozen solutions of PDADMAC and TAM. The final section gives a summary of the conclusions drawn from the experimental findings.

Materials and methods

Materials

The spin probes used in this study (Scheme 1) were Fremy's salt dianion (potassium nitrosodisulfonate, FS) of technical grade (ICN Biomedicals) and triarylmethyl trianion sodium salt (TAM, a gift from Nycomed Innovations AB, Sweden) of unknown purity. As cationic polyelectrolyte we chose poly(diallyldimethylammonium chloride) (PDADMAC) with an M_W of 240,000 (Polysciences, Inc.). All chemicals were used as received.

As solvent systems we chose deionized Milli-Q-water (permittivity $(\epsilon_r) = 80$ at 293 K), 66 wt% glycerol/34 wt% water (made from 87 wt% glycerol/water mixture, Fluka, density $(\rho) \approx 1.17$ g mL^{-1}, approximate $\epsilon_r = 57$ at 293 K). Solutions containing FS spin probe were adjusted to pH > 8 by addition of small amounts of KOH. This was necessary to improve stability of FS to chemical degradation. Spin probe concentrations were fixed at 0.5 mM for FS ions and at 0.4 mM for TAM; polyelectrolyte concentration was varied from 4 mM (in repeat units) to 140 mM. This is necessary to exclude all effects that could result from simply altering the initial bulk concentration of the ion of spectroscopic interest. No ion exchange was carried out, and the multivalent spin probes have been shown [15] to partly replace the original PDADMAC counterions (chloride) as expected from simple counterion condensation theory. Data are presented as a function of the ratio R of spin probes to polymer repeat units in order to avoid ambiguities arising from the broad molecular weight distribution (polydispersity index $M_W/M_N \approx 2.5$).

EPR spectroscopy and simulations

CW EPR [13] spectra in solution at X-band (9.7 GHz) were measured on a Bruker ELEXSYS 580 spectrometer using an AquaX inlet and a rectangular cavity (4103TM, Q-values typically 3000). The temperature during these measurements was 293 K. EPR spectra at high-field/high-frequency (W-band, ≈94 GHz) were recorded on a Bruker ELEXSYS 680 spectrometer with a Bruker TeraFlex probehead. Sample volumes of 1–3 μL were placed into round-bottomed tubes homemade from Suprasil capillary material (inner diameter 0.7 mm, outer diameter 0.87 mm, Wilmad Corp., USA). The tubes were then sealed with fast-drying glue (Loctite 454). Measurements at $T = 80$ K were performed by cooling with liquid nitrogen using an Oxford cryostat and cooling system.

Fitting of spectra subjected to dipolar broadening was performed with a home-written program in MATLAB (v.6.1, The Mathworks, Inc.) by minimizing the root-mean-square deviation of simulated from experimental spectra. The simulated spectrum was computed by convolution of an unbroadened reference spectrum with a superposition of Pake patterns corresponding to a Gaussian distribution of distances [20, 21, 22, 23]. The Pake patterns themselves were taken from a precomputed table corresponding to intermolecular distances between 0.1 and 5 nm in increments of 10^{-3} nm [20].

EPR spectroscopy of charged spin probes in solutions of PDADMAC

In previous systematic studies of solutions containing PDADMAC as a polyelectrolyte and FS or TAM spin probes as tracers for counterions [15, 16, 17], we have found that in the regime of counterion condensation, multivalent spin probes are transiently attached to charges on the PDADMAC chain with a lifetime of this site-bound state of less than a nanosecond. For this fast exchange between the site-bound and territorially bound states, the term *dynamic electrostatic attachment* (DEA) was introduced [15].

To characterize DEA in detail, viscosity and permittivity of the solvent were varied by performing these experiments in water and mixtures of water with ethanol, *N*-methylpropionamide, and glycerol. Variation of these macroscopic solvent properties did not result in the effects expected from simple Manning theory of counterion–polyion interaction. It was rather found that the solvent *structure* plays a crucial role, that is, that organic solvents may preferentially solvate the hydrophobic PDADMAC chain backbone, and may thus prevent a chain collapse that occurs in water [15].

Upon increase of the spin probe/polyelectrolyte ratio R (i.e., decrease of PDADMAC concentration), we observed increasing line broadening in CW EPR spectra, which particularly affected the outer wings of the lines. This broadening could be explained by increased exchange interaction between individual ionic spin probes due to a higher frequency of counterion–counterion collision. The broadening is thus directly related to the enhanced local concentration of counterions close to the

polyelectrolyte chain. A quantitative analysis of this aspect of counterion binding indicated that in PDADMAC solutions the distributions of nanosized organic TAM trianions and small inorganic FS dianions are qualitatively different. For TAM trianions, the experimental data could be consistently interpreted by assuming that with increasing TAM/PDADMAC ratio R an abrupt change takes place from a regime in which the polyelectrolyte chains strongly overlap (high concentration, $R < 0.03$) to a regime in which individual polyelectrolyte chains dominate ($R > 0.03$). The former regime may be dominated by TAM molecules building transient physical crosslinks between PDADMAC chains, while the latter regime may consist of TAM molecules interacting with only a single polyelectrolyte chain, which does not, however, imply that there is no long-range interaction between individual chains.

No such crosslinking ability was found for the smaller and more hydrophilic FS dianions. While DEA of FS ions appears to involve only one of the charge-bearing ammonium groups on PDADMAC at any given time [17], force field simulations (MMFF94 as implemented in SPARTAN) of one TAM trianion with an excerpt 16 PDADMAC repeat units including original counterions suggest that the polyelectrolyte chain can easily deform in order to attach the three anionic centers of TAM to non-neighbor repeat units (see Figure 2). For longer chains, connection of more remote repeat units should occur yet more easily.

By additional pulse EPR experiments, information on the spin probe distribution *along polyelectrolyte chains* could be gained. For the FS counterion this could be achieved by the double electron–electron resonance (DEER) experiment, which is sensitive to distances between spin probes in the range from approximately 1.5 to 8 nm. Within this range we did not find a well-defined characteristic distance of FS counterions bound to a PDADMAC chain. Rather, the DEER data could be simulated by assuming two states of spin probes, one corresponding to a homogeneous *spatial* (3-dimensional) distribution of counterions in the bulk and the other to a homogeneous *linear* (1-dimensional) distribution along locally extended PDADMAC chain segments. Furthermore, this analysis suggested that PDADMAC chains form locally elongated structures of a size of at least approximately 5 nm [17].

Against this background, the present work now describes results from pulse EPR experiments on systems of TAM/PDADMAC at high-field/high-frequency (W-band, ≈94 GHz). These experiments probe the local TAM counterion concentration in frozen solution samples of TAM/PDADMAC and can thus deliver further information on the local structure of such systems.

Distribution of network-forming counterions

Unlike the divalent FS ion that is a rather small inorganic molecule, the TAM trianion (see Scheme 1) represents a class of rigid, triangular-shaped organic molecules with their structure deviating strongly from that of usual polyelectrolyte counterions such as chloride ions. In numerous studies, such large organic molecules have been shown to interact with oppositely charged polyions not only by electrostatic but also by hydrophobic interactions [7, 24]. TAM in particular consists of three aromatic structural units and of twelve short hydroxyethyl moieties, which all might seek interaction with large organic macromolecules. The well-defined, rigid structure of this molecule and especially the triangular arrangement of charges with an intercharge distance of 1 nm raise the expectation that it might be used as a structural guiding block for supramolecular assemblies.

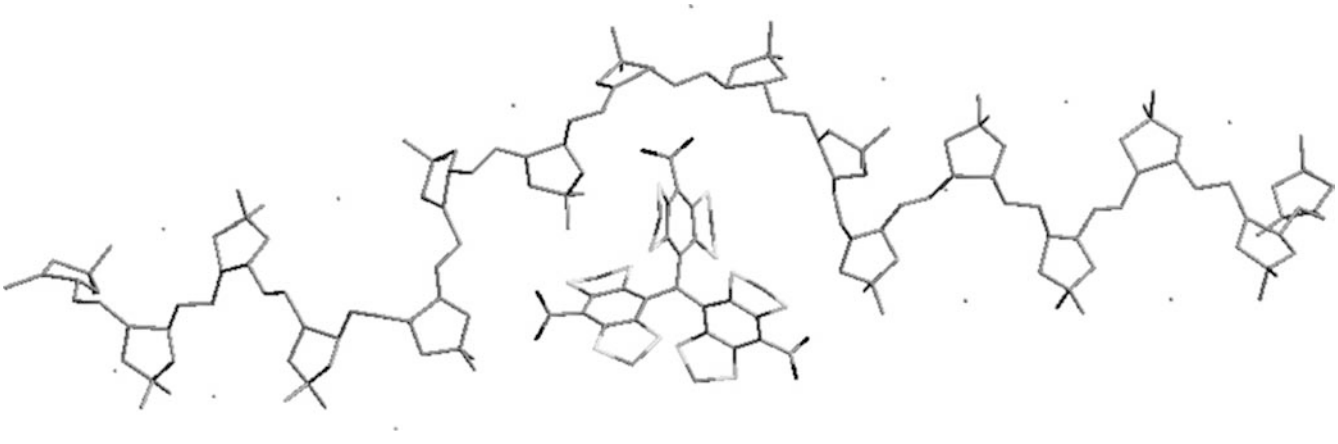

Fig. 2 Geometry-optimized structure (force-field simulation, MMFF94) of the core of one TAM trianion and a short PDADMAC chain (16 repeat units, including counterions). Upon electrostatic attachment of TAM the local chain structure is deformed and a "binding pocket" is formed. Note that the 12 sidegroups of the TAM radical are not shown for clarity

TAM spin probe distributions characterized from broadening of high-field ESE-detected spectra

Line broadening in liquid-state EPR spectra is a useful source of semi-quantitative information on proximity of spin probes, but is not so easily interpreted in terms of a distance distribution. This is because diffusion dynamics and spin dynamics proceed on the same time scale, so that a sizeable number of parameters are involved, which cannot be determined exactly by independent experiments. Such liquid-state spectra are thus better analyzed in terms of scaling laws than in terms of absolute distances. In contrast, the distance distribution can be derived on the basis of first principles from dipole–dipole coupling between spins in the solid state [25, 26]. Furthermore, unpaired electron spin density is located predominantly (≈50%) on the central carbon atom of the TAM trianion, as was found by density-functional calculations (Titan v1.0, B3LYP density functional, 6–31* basis set) [21]. Hence, measurements of interspin distances of TAM radicals in the solid state are, to a good approximation, measurements of the distance between the centers of TAM trianions.

Solid-state structure is related to solution structure in such systems, which attain a glassy state on shock freezing. To a good approximation, local solid-state structure then corresponds to the average over the ensemble of local structures at the glass transition temperature, where during shock freezing the system ceases to adapt to thermodynamic equilibrium. To prepare such glassy samples, we use a mixture of glycerol/water (2:1 v/v) as a solvent, which was also studied in liquid-state experiments [16]. A series of samples containing the TAM trianions and PDADMAC polyelectrolyte in the range of concentration ratios R between 0.0028 and 0.1 was investigated by ESE-detected EPR at W-band (≈94 GHz) EPR frequency and a temperature of 80 K. By performing these experiments at high frequency we avoid complications due to proton spin-flip transitions that are prominent at X-band frequencies, depend on polyelectrolyte concentration, and will be discussed elsewhere. In Fig. 3, high-field/high-frequency electron spin echo (ESE)-detected EPR spectra for TAM at three different R values [without PDADMAC, $R = 0.0028$ (140 mM PDADMAC), and $R = 0.1$ (4 mM PDADMAC)] are shown. The apparent asymmetry of the spectra can be assigned to anisotropy of the g tensor [13], as proposed by Griffin and coworkers [27] on the basis of ESE-detected spectra recorded at 139.5 GHz.

The spectra in Fig. 3 clearly show line broadening that increases with increasing R. From these spectra, information on the distribution of distances between TAM trianions can be extracted in a fairly simple approach by fitting broadened spectra $V_{sim}(B_0)$, which are simulated by convolution of a reference spectrum

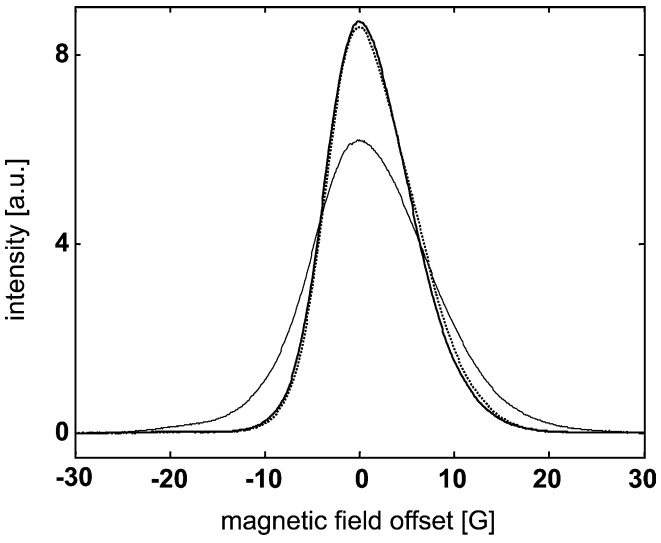

Fig. 3 Representative ESE-detected, field-swept EPR spectra (W-band, ≈94 GHz) of 0.4 mM TAM + PDADMAC in frozen glycerol/water solution ($T = 80$ K) at three R-values. *Dotted line* TAM without polyelectrolyte; *bold solid line* $R = 0.0028$; *thin solid line* at $R = 0.1$. Note the asymmetry of the spectra

$V_{ref}(B_0)$ with a dipolar broadening function, to the experimental spectra [22, 23]. As the reference spectrum we use the spectrum of the $R = 0.0028$ sample (bold solid line in Fig. 3) rather than the spectrum in the absence of PDADMAC, as the line shape is sensitive to interactions of the spin probe with direct neighbors, for instance to the polarity and hydrogen-bonding ability of the matrix [13]. The dipolar broadening function corresponds to a Gaussian distribution of distances with two parameters: i) the mean distance $\langle r_{dip} \rangle$ between unpaired electrons (centers of TAM ions) and ii) the width of the Gaussian distribution Δr_{dip}.

Assuming the same dipolar broadening function for all TAM trianions did not result in good fits of the experimental spectra (data not shown). This finding strongly suggests that the distribution of TAM ions is heterogeneous, as might also be expected from a Manning-like picture that supposes the existence of site-bound, territorially bound, and free counterions. The simplest model that does fit our data assumes the existence of two fractions, a fraction f with significant dipolar broadening (clustered counterions) and a fraction 1-f with insignificant broadening (dilute counterions). As the reference spectrum pertains to high polyelectrolyte concentration, the latter fraction can be assigned to TAM trianions that are homogeneously distributed in the bulk of overlapping polyelectrolyte chains. For the discussion of network formation, the former fraction is of greater interest.

This simple picture results in a spectrum that can be described by a superposition of two spectral components

referring to the two fractions of counterions, clustered (dipolar broadened) and dilute (reference):

$$V_{\mathrm{sim}}(B_0) = (1-f)\cdot V_{\mathrm{ref}}(B_0) + f \cdot V_{\mathrm{dip}}(B_0) \quad (1)$$

The parameters $\langle r_{\mathrm{dip}}\rangle$, Δr_{dip}, and f were fitted by minimizing the root-mean-square (rms) deviation between $V_{\mathrm{sim}}(B_0)$ and the experimental spectra. Note that in this approach only the first peak of the distance distribution stemming from the closest neighbor trianions is analyzed. Due to the r^{-3}-dependence of the dipolar coupling this is a good approximation, as dipolar broadening to all other electron spins located farther away is negligible.

As an example of such a fit, Fig. 4 shows the spectrum at $R = 0.05$ and the residual obtained by subtraction of the simulated from the experimental spectrum. Fits throughout the whole R range were of similar quality. In Fig. 5, the extracted mean distances $\langle r_{\mathrm{dip}}\rangle$ and fractions of clustered trianions f are plotted versus the counterion to repeat unit ratio R. The width $\Delta r_{\mathrm{di}\ p}$ of the distance distribution varied between 0.1 and 0.5 nm. However, as the simulated spectra are rather insensitive to Δr_{dip} in this range, we discuss only changes in f and $\langle r_{\mathrm{dip}}\rangle$.

We find that throughout the range $0.01 < R < 0.1$, the mean distance between an observer TAM trianion and its closest neighbor trianion decreases only slightly from approximately 1.6 nm to about 1.4 nm, and even for the highest polyelectrolyte concentration the distance is still as small as approximately 2.0 nm (Fig. 5a). A change in polyelectrolyte concentration results mainly in a change of the fraction f of trianions that are situated within clusters.

The same analysis was attempted for X-band (≈9.6 GHz) ESE-detected EPR spectra of FS/PDADMAC samples, but did not result in good fits of experimental spectra for $R > 0.03$. Failure of the method in this case may be attributed to the much shorter $\langle r_{\mathrm{dip}}\rangle$ for the smaller FS dianions, which leads to additional broadening by through-solvent exchange coupling [28]. We may, however, compare the results for TAM trianions from the present work to DEER data for FS [17] that pertain to a similar length scale. The main difference between the two systems lies in the dependence of the closest ion-to-ion distance $\langle r_{\mathrm{dip}}\rangle$ on polyelectrolyte concentration. In the system FS/PDADMAC this parameter markedly depends on R, whereas it is almost constant in the TAM/PDADMAC system. In the following section, we discuss this finding with respect to polyelectrolyte network formation.

Discussion

Zip-like clustering of TAM crosslinks

The shortest mean distance between the centers of TAM ions is found to be 1.4 nm at $R = 0.1$ corresponding to the lowest polyelectrolyte concentration. This value coincides remarkably well with the minimum distance

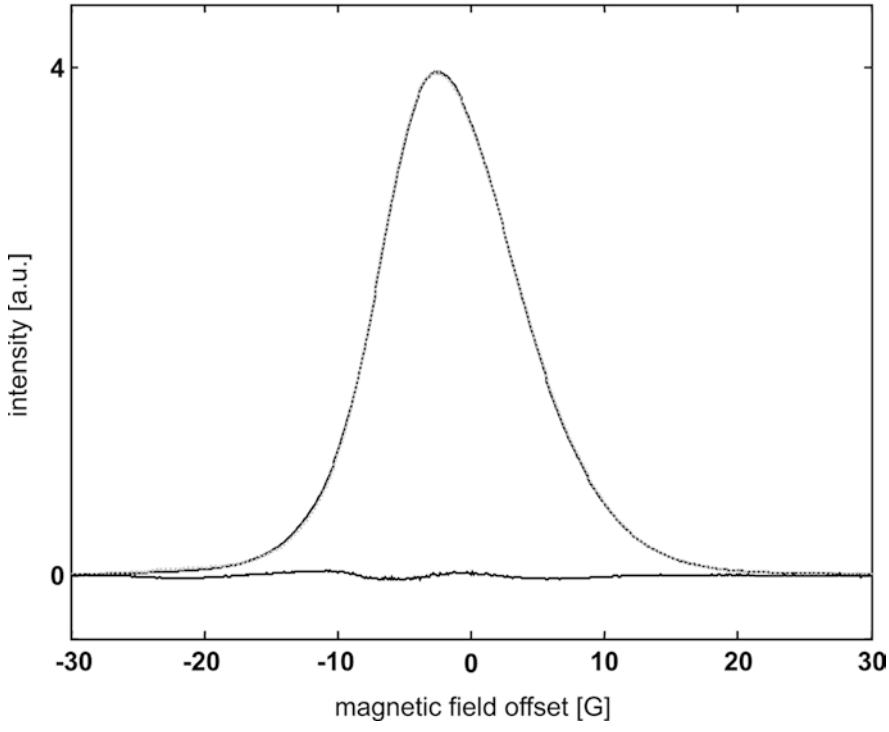

Fig. 4 ESE-detected, field-swept EPR spectrum (W-band, ≈94 GHz) of TAM + PDADMAC in frozen glycerol/water solution ($T = 80$ K) at $R = 0.05$ (*solid black line*) and simulation by the convolution approach explained in the text (*superimposed dotted gray line*). *Upper trace* experimental/simulated spectra; *lower trace* fit residual of a simulated spectrum with parameters $f = 0.42$, $\langle r_{\mathrm{dip}}\rangle = 1.5$ nm, $\Delta r_{\mathrm{dip}} = 0.3$ nm

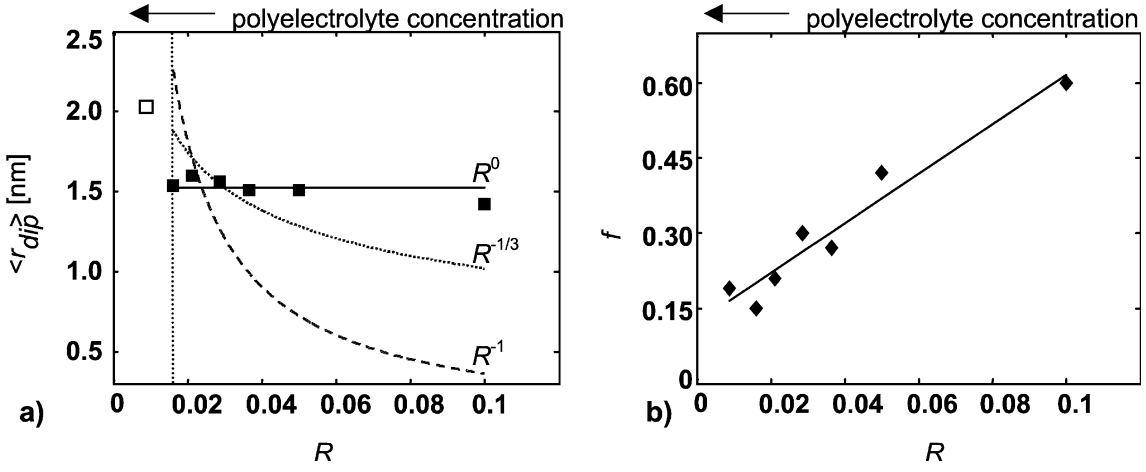

Fig. 5a,b Dependence of the mean distance $\langle r_{dip} \rangle$ (**a**) and fraction f of clustered TAM counterions (**b**) in frozen PDADMAC solutions in glycerol/water on ratio R between the concentrations of TAM trianions and PDADMAC repeat units ($T = 80$ K). **a** Experimental data (*black squares*) and dependences expected from models assuming a constant mean distance, that is, scaling with R^0 (*solid line*), scaling with $R^{-1/3}$ (*dotted line*), and scaling with R^{-1} (*dashed line*). The first data point deviates from the trend (*open square*), only data *right* from the *vertical dotted line* ($R = 0.016$) are included in the fit **b** experimental data (*black diamonds*) and linear fit ($f = 4.94R + 0.12$)

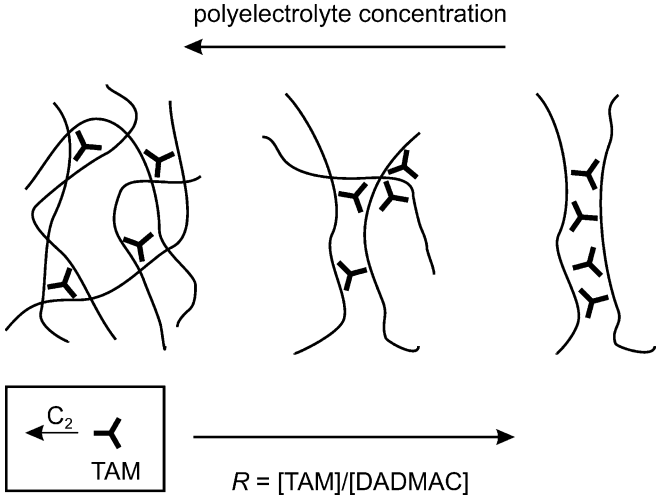

Fig. 6 Schematic visualization of clustered counterion binding. With increasing R, TAM trianions are increasingly attached to sites close to each other, which explains the increase in f in Fig. 5b. The *inset* indicates one of the C_2 symmetry axes of the TAM trianion

expected for an approach of two TAM trianions along one of the C_2 molecular axes (see Scheme 1). We may thus conclude that at low polyelectrolyte concentration, a significant fraction of TAM trianions are situated in densely packed clusters. The fact that $\langle r_{dip} \rangle$ changes only slightly between $R = 0.016$ and $R = 0.1$ implies that the inner structure of the clusters is almost invariant. To test for the significance of this statement, we may compare the experimental dependence of $\langle r_{dip} \rangle$ on R to expectations for a homogeneous linear distribution along a stretched polyelectrolyte chain and for a homogeneous spatial distribution in a polyelectrolyte coil. As R is inversely proportional to the concentration of repeat units, $\langle r_{dip} \rangle$ should scale with R^{-1} in the former case and with $R^{-1/3}$ in the latter case. The best adjustments to these models (stretched chains: rms of 1.62, dashed line in Fig. 5a; polyelectrolyte coil: rms of 0.59, dotted line in Fig. 5a) are clearly at variance with the experimental data. The constant mean distance clearly provides the best, yet not perfect fit among these three models (rms of 0.14, solid line). The simplest model for the distribution of TAM counterions is thus that fraction f resides in clusters where the individual counterions have close lateral contact, while fraction 1-f is homogeneously distributed over the coils outside the clusters. The latter fraction also interacts with the polyelectrolyte, which explains the slightly different line shapes in the absence of PDADMAC and at high concentrations of PDADMAC.

The steady increase of fraction f with increasing R (Fig. 5b) can be analyzed in a similar manner as the decrease of the concentration of spatially distributed FS dianions and the increase of their linear spin density that was deduced from DEER data for the FS/PDADMAC system [17]. At low R-values and thus high PDADMAC concentrations, the polyelectrolyte chains overlap and the TAM trianions can have hydrophobic and electrostatic contact while being diluted in the bulk. With increasing R the number of existing sites for such favorable attachment decreases, and the TAM trianions have to organize their preferred environment themselves. Based on CW/FT EPR measurements in liquid solution [15, 16] it has been postulated that TAM acts as a physical crosslinking agent, which agrees with this interpretation. The idea is visualized in Fig. 6, where the system is sketched at three different R-values. Note that the schematically drawn chain segments do not necessarily belong to different PDADMAC chains.

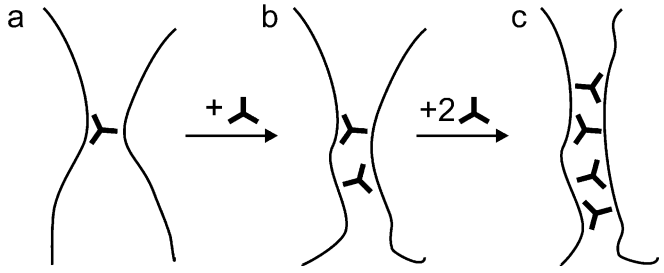

Fig. 7a–c Schematic representation of the proposed zip-like formation of domains of polyelectrolyte due to physical crosslinking by tristar-shaped TAM counterions. **a** The first TAM ion connects two polyelectrolyte chains or two domains of the same chain. **b** Close to the attachment site of the first ion a favorable site for attachment of a second ion is formed. **c** The two chains or chain segments are now nearly parallel and predisposed to take up further TAM ions

If in the absence of the nanosized trianions, no favorable attachment sites exits, such sites could be formed by a zip-like crosslinking that resembles cooperative binding. This is because once one such a junction has been established, other favorable sites are preformed. The effect arises from the proximity of the chains after formation of the first physical crosslink, but may be enhanced by a geometrical predisposition to form new connections: an isolated polyelectrolyte chain is expected to be locally stretched due to electrostatic repulsion and may thus act as a topological constraint. A possible mechanism of such cooperative binding at a given ratio R is schematically depicted in Fig. 7.

This zip-like network formation can be discussed in terms of entropy and enthalpy gains and losses. In general, electrostatic attachment increases entropy by the release of a larger number of monovalent counterions. In the case at hand, this entropy gain is partially offset by the entropy loss due to the loss of conformational freedom of the polyelectrolyte chains. An unfavorable enthalpy increase is expected due to the approach of two chains or chain segments with total positive charges. This is counteracted by partial charge compensation by attachment of trianions and possibly by the preferential interaction of the hydrophobic, voluminous organic TAM ions (with twelve hydroxyethyl side chains) with the hydrocarbon backbone of PDADMAC. Such a support of counterion attachment by hydrophobic interactions has been discussed previously in the context of organic dyes [7, 24]. A quantitative theoretical analysis of these thermodynamic issues is hampered by the complexity of the problem, which involves several factors such as electrostatic interactions, hydrophobic interactions, polymer chain conformation, and selective solvation.

The picture sketched above somewhat resembles the formation of thermoreversible gels, which has been studied extensively [7, 29, 30]. This is generally acknowledged to be a two-step process involving initial creation of small macromolecular aggregates and subsequent further aggregation of these molecular clusters. Despite the heterogeneity of the two-step process, during gel formation, the system remains macroscopically homogeneous [7]. Although the situation is somewhat different in the case of TAM/PDADMAC, one may nonetheless deduce that by analogy to the aggregated and non-aggregated states in thermoreversible gels, in the investigated system there may be isolated and clustered TAM crosslinks at any time even at low ratios of spin probe/polyelectrolyte. The overall system remains homogeneous on long length scales.

In light of the general scheme shown in Fig. 1, network formation induced by the tristar-shaped nanosized TAM trianions resembles bundling of rigid rod-like molecules. At least this would be expected as a consequence of the increased intrinsic stiffness due to charge repulsion, as proposed by the worm-like chain model of polyelectrolytes first developed by Odijk, Skolnick, and Fixman (OSF) [31]. The polyelectrolyte chains may thus compact only to the minimum extent that is necessary to accommodate the given amount of TAM counterions.

Summary

In this study, the approach to use charged spin probes as tracers for counterions of PDADMAC polyelectrolytes was expanded from small, inorganic spin probes to large, tristar-shaped organic molecules of the triarylmethyl (TAM) class. By simulation of high-field/high-frequency electron spin echo (ESE)-detected EPR spectra information on the distance distribution of TAM radicals within frozen solutions of PDADMAC could be obtained.

Even in samples that contained as little as one TAM trianion per 100 PDADMAC repeat units, a non-negligible fraction of these ions are in close contact ($\approx$1.5 nm) with each other. With increasing ratio of TAM/PDADMAC, the closest distance remains constant within experimental precision, while the fraction of clustered multivalent counterions increases. These findings suggest that the large organic TAM spin probes can act as network-inducing agents in solutions of PDADMAC polyelectrolyte. Taking into account the topology and intrinsic stiffness of the polyelectrolyte chains, a zip-like cooperative binding effect of TAM ions is proposed to explain such network formation.

Acknowledgments We thank Nycomed Innovations AB, Sweden, for generously supplying us with the TAM radical used in this study and C. Bauer for technical support. Financial support from the priority program "High-Field EPR in Biology, Chemistry and Physics" (SPP 1051) by the Deutsche Forschungsgemeinschaft (DFG) is gratefully acknowledged.

References

1. Mark JE (ed) (1982) Polymer networks, advances in polymer science vol 44. Spirnger-Verlag, Berlin Heidelberg New York
2. Pietralla M, Kilian H-G (eds) (1987) Permanent and transient networks, progress in colloid and polymer science vol 75. Steinkopff-Verlag, Darmstadt
3. Yan Q, de Pablo JJ (2003), Phys Rev Lett 91:018301–1. DOI 10.1103/PhysRevLett.91.018301
4. Ogawa S, Decker EA, McClements DJ (2003) J Agric Food Chem 51:2806
5. Lee SH (2000) Polymer J 32:716
6. Peppas NA, Huang Y, Torres-Lugo M, Ward JH, Zhang J (2000) Annu Rev Biomed Eng 2:9
7. Dautzenberg H, Jaeger W, Kötz J, Philip B, Seidel C, Stscherbina D (1994) Polyelectrolytes–formation, characterization and application. Carl Hanser Verlag, Munich
8. Kötz J, Kosmella S, Beitz T (2001) Prog Polym Sci 26:1199
9. Rubinstein M, Colby RH (2003) Polymer physics. Oxford University Press
10. Liu H, Skibinska L, Gapinski J, Patkowski A, Fischer EW, Pecora R (1998) J Chem Phys 109:7556; Skibinska L, Gapinski J, Liu H, Patkowski A, Fischer EW, Pecora R (1999) J Chem Phys 110:1794
11. Bockstaller M, Köhler W, Wegner G, Vlassopoulos D, Fytas G (2001) Macromolecules 34:6359
12. Fischer EW (1957) Z Naturforsch 12A:753
13. Atherton NM (1993) Principles of electron spin resonance. Ellis Horwood, New York
14. Tsagaropoulos G, Kim JS, Eisenberg A (1996) Macromolecules 29:2222
15. Hinderberger D, Jeschke G, Spiess HW (2002) Macromolecules 35:9698
16. Hinderberger D, Spiess HW, Jeschke G (2004) Macromol Symp, in press
17. Hinderberger D, Spiess HW, Jeschke G (2004) J Phys Chem B 108:9698
18. Ardenkjaer-Larsen JH, Laursen I, Leunbach I, Ehnholm G, Wistrand LG, Petersson JS, Golman K (1998) J Magn Res 133:1
19. Yong L, Harbridge J, Quine RW, Rinard GA, Eaton SS, Eaton GR, Mailer C, Barth E, Halpern HJ (2001) J Magn Res 152:156
20. Schweiger A, Jeschke G (2001) Principles of pulse electron paramagnetic resonance. Oxford University Press
21. Hinderberger D (2004) Polyelectrolytes and their counterions studied by EPR spectroscopy. Doctoral dissertation, Mainz
22. Rabenstein MK, Shin YK (1995) Proc Natl Acad Sci 92:8239
23. Gross A, Columbus L, Hideg K, Altenbach C, Hubbell WL (1999) Biochemistry 28:10324
24. Dawydoff W, Linow KJ, Philipp B (1991) Acta Polym 42:592; Acta Polym 42:646
25. Jeschke G, Koch A, Jonas U, Godt A (2002) J Magn Res 155:72
26. Jeschke G (2002) ChemPhysChem 3:927
27. Farrar CT, Hall DA, Gerfen GJ, Rosay M, Ardenkjaer-Larsen JH, Griffin RG (2000) J Magn Res 144:134
28. Jeschke G (2002) Macromol Rapid Comm 23:227
29. Rees DA (1969) Carbohydr Chem 24:267
30. Dawydoff W, Linow KJ, Philipp B (1984) Nahrung 28:241
31. Odijk J (1977) J Polym Sci Polym Phys 15:477; Skolnick J, Fixman M (1977) Macromolecules 10:944